A role for UDP-glucose glycoprotein glucosyltransferase in expression and quality control of MHC class I molecules

Wei Zhang[a,b], Pamela A. Wearsch[b,c], Yajuan Zhu[a,b], Ralf M. Leonhardt[b,c], and Peter Cresswell[a,b,c,1]

Departments of [c]Immunobiology and [a]Cell Biology, [b]Howard Hughes Medical Institute, Yale University School of Medicine, New Haven, CT 06520-8011

Contributed by Peter Cresswell, February 14, 2011 (sent for review January 5, 2011)

UDP-glucose:glycoprotein glucosyltransferase 1 (UGT1) serves as a folding sensor in the calnexin/calreticulin glycoprotein quality control cycle. UGT1 recognizes disordered or hydrophobic patches near asparagine-linked nonglucosylated glycans in partially misfolded glycoproteins and reglucosylates them, returning folding intermediates to the cycle. In this study, we examine the contribution of the UGT1-regulated quality control mechanism to MHC I antigen presentation. Using UGT1-deficient mouse embryonic fibroblasts reconstituted or not with UGT1, we show that, although formation of the peptide loading complex is unaffected by the absence of UGT1, the surface level of MHC class I molecules is reduced, MHC class I maturation and assembly are delayed, and peptide selection is impaired. Most strikingly, we show using purified soluble components that UGT1 preferentially recognizes and reglucosylates MHC class I molecules associated with a suboptimal peptide. Our data suggest that, in addition to the extensively studied tapasin-mediated quality control mechanism, UGT1 adds a new level of control in the MHC class I antigen presentation pathway.

antigen processing | chaperones

Major histocompatibility complex (MHC) class I-mediated antigen presentation is critical for adaptive immune responses to intracellular pathogens. MHC class I assembly and peptide loading constitute a specialized case of glycoprotein folding, using general chaperones and enzymes involved in the endoplasmic reticulum (ER) quality control machinery as well as MHC class I-specific cofactors. Like other glycoproteins, MHC class I heavy chains (HCs) are modified during translocation by asparagine (N)-linked glycosylation with the glycan $Glc_3Man_9GlcNAc_2$. After the first two glucose residues are trimmed by glucosidases I (GlsI) and II (GlsII), the monoglucosylated ($Glc_1Man_9GlcNAc_2$) glycan interacts with the lectin chaperone calnexin (CNX) for oxidative folding (1). The maturing HCs are partially stabilized by β_2-microglobulin (β_2m) association, and the HC/β_2m dimers are recruited by the second lectin chaperone calreticulin (CRT) into the peptide loading complex (PLC) via their monoglucosylated glycans (2, 3). The PLC is composed of the HC/β_2m dimer, CRT, the transporter associated with antigen processing (TAP), and a disulfide-linked tapasin-ERp57 conjugate (reviewed in ref. 4). It facilitates peptide loading onto MHC class I molecules and functions in quality control by retaining empty and suboptimally loaded MHC class I molecules in the ER.

The glycosylation status of ER MHC class I molecules is highly regulated. Monoglucosylation is not detectable in free human MHC class I HCs (5), whereas PLC-associated HCs are virtually all monoglucosylated (3, 5). Inhibiting deglucosylation of the monoglucosylated glycan prolongs the interaction of MHC class I molecules with the PLC (3, 6), and, in vitro, GlsII can trim the monoglucosylated glycans of free HCs but not PLC-associated HCs (3). This suggests that only when MHC class I molecules dissociate from the PLC are the glucose residues accessible to GlsII. Once the final glucose is removed, MHC class I molecules can no longer associate with the PLC because their recruitment is dependent on the monoglucosylated glycan/CRT interaction (3, 7). This leads to the question of whether a mechanism exists that can rescue suboptimally loaded, unstable MHC class I molecules that have dissociated prematurely from the PLC.

A potential candidate for such a mechanism is the soluble enzyme UDP-glucose:glycoprotein glucosyltransferase 1 (UGT1), which can selectively reglucosylate an N-linked glycan according to the conformation of the protein bearing it. After sequential trimming of glucoses by GlsI and GlsII, interaction of monoglucosylated glycoproteins with CNX and/or CRT prevents folding intermediates from premature export, aggregation, or destruction, and recruits the oxidoreductase ERp57 to assist disulfide bond formation (8). GlsII further removes the final glucose and liberates glycoproteins from the CNX/CRT cycle. ER export is prevented until the glycoproteins have achieved their correct conformation. If this does not occur, UGT1, which is restricted to the ER and pre-Golgi compartment (5), recognizes hydrophobic patches near a $Man_9GlcNAc_2$ structure and transfers a glucose residue from UDP-glucose to regenerate $Glc_1Man_9GlcNAc_2$, restoring recognition by CNX and CRT (9).

UGT1 has striking substrate specificity: it prefers near-native molten globule-like folding intermediates and orphan subunits, and ignores native or extensively misfolded proteins (10–12). How this specificity is accomplished remains unclear. Two different systems have been used to study UGT1, both with their own advantages and limitations. One is a cell-free system examining the activity of purified UGT1 using simple soluble substrates. Although informative, cell-free studies fail to mimic the broader context of the CNX/CRT cycle. The second system uses intact UGT1-deficient cell lines, but has the major difficulty that direct and indirect effects are difficult to differentiate, as UGT1 works on a broad range of substrates. Here we investigate whether UGT1 acts as a quality control factor for MHC class I antigen presentation using both cell-free and cell-based assays. Using UGT1-deficient mouse embryonic fibroblasts (MEFs) reconstituted or not with UGT1, we find that despite seemingly unaffected PLC formation, in the absence of UGT1, MHC class I surface expression is reduced, its maturation and assembly are delayed, and peptide selection is impaired. In addition, we show using purified soluble components that UGT1-dependent reglucosylation of the N-linked glycan of MHC class I/β_2m dimers associated with high-affinity peptides is reduced by more than 90% compared with dimers associated with suboptimal peptides. These data indicate that UGT1 acts as a checkpoint in the quality control of the MHC class I antigen presentation pathway.

Author contributions: W.Z., P.A.W., and P.C. designed research; W.Z. and P.A.W. performed research; W.Z., P.A.W., Y.Z., R.M.L., and P.C. analyzed data; and W.Z. and P.C. wrote the paper.

The authors declare no conflict of interest.

Freely available online through the PNAS open access option.

[1]To whom correspondence should be addressed. E-mail: peter.cresswell@yale.edu.

This article contains supporting information online at www.pnas.org/lookup/suppl/doi:10.1073/pnas.1102527108/-/DCSupplemental.

Results

PLC Assembly Is Not Affected by the Absence of UGT1. To investigate the role of UGT1 in MHC class I antigen presentation, we stably expressed mouse UGT1 in UGT1-deficient MEFs (13) using the retrovirus vector MSCV-UGT1-IRES-Thy1.1, or empty MSCV-IRES-Thy1.1 vector as a control, establishing cell lines henceforth referred to as KO.UGT1$^+$ and KO.UGT1$^-$, respectively. UGT1 expression was confirmed by Western blotting (Fig. 1*A*) and did not affect the steady-state levels of TAP, CRT, ERp57, or tapasin (Fig. 1*B*). To assess PLC formation, we isolated it by immunoprecipitation with a TAP1-specific antibody and detected the individual components by Western blotting following SDS/PAGE (Fig. 1*B*). As shown, CRT, ERp57, tapasin, and MHC class I molecules appeared to be incorporated into the PLC normally. The only significant difference observed between the UGT1-positive and UGT1-negative cells was the glycosylation pattern of the H2-K^b HCs (Fig. 1*B*). In KO.UGT1$^+$ cells, more of the K^b molecules were in the heavily glycosylated post-ER form (the upper band), whereas KO.UGT1$^-$ cells contained relatively higher levels of HCs with unprocessed glycans. The formation of the ERp57-tapasin conjugate, which recruits/stabilizes MHC class I molecules and edits the peptide repertoire, was unaffected by the absence of UGT1 (Fig. 1*C*). There was no difference in the intracellular distribution of the MHC class I molecules between the two cells (Fig. S1).

MHC Class I Surface Expression and Antigen Presentation Are Impaired in the Absence of UGT1. The surface levels of K^b and D^b, determined by flow cytometry, were reduced in UGT1-deficient MEFs by 35% and 40%, respectively, compared with the levels in WT cells, but were partially rescued by restoration of UGT1 expression (KO.UGT1$^+$; Fig. 2*A*). To examine the effect on antigen presentation, we transfected a vector encoding GFP-ubiquitin-SIINFEKL into KO.UGT1$^+$ and KO.UGT1$^-$ cells. After translation, the SIINFEKL peptide is released from GFP-ubiquitin by the ubiquitin C-terminal hydrolase in the cytosol, and GFP expression gives a relative measure of protein expression (14). The surface presentation of SIINFEKL by K^b was analyzed by flow cytometry using the mAb 25-D1.16, which recognizes K^b/β_2m dimers associated with the SIINFEKL peptide. Cells were arranged in eight groups according to GFP expression, and the mean level of 25-D1.16 binding in each group was plotted against the mean GFP level (Fig. 2*B*). The data clearly show that KO.UGT1$^+$ cells are more efficient in presenting SIINFEKL than the UGT1-negative control. In each case, at high antigen doses the number of surface K^b/SIINFEKL complexes reached a plateau, perhaps because of limitations in peptide transport, loading, or ER export rates, but the defect in SIINFEKL presentation seen in the absence of UGT1 was not overcome.

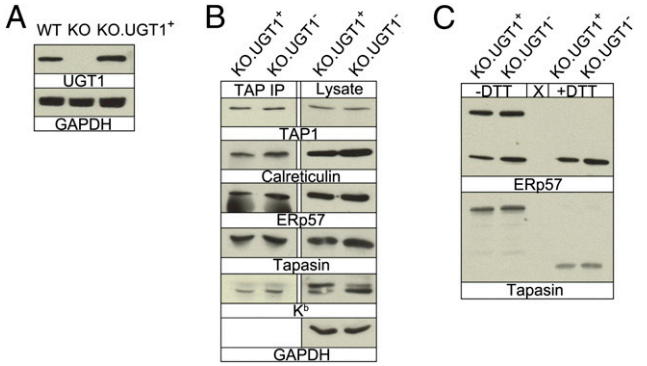

Fig. 1. PLC formation is not affected by the absence of UGT1. (*A*) WT MEFs, UGT1-deficient MEFs (KO), and UGT1-deficient MEFs expressing mouse UGT1 (KO.UGT1$^+$) were blotted for UGT1 or GAPDH as a loading control. (*B*) TAP1 immunoprecipitates (*Left*) or the whole-cell lysate (*Right*) from KO.UGT1$^+$ or KO.UGT1$^-$ were blotted for TAP, CRT, ERp57, tapasin, K^b, and GAPDH. (*C*) Lysates from KO.UGT1$^+$ and KO.UGT1$^-$ were resolved by SDS/PAGE under nonreducing (–DTT) or reducing (+DTT) conditions and blotted for ERp57 and tapasin.

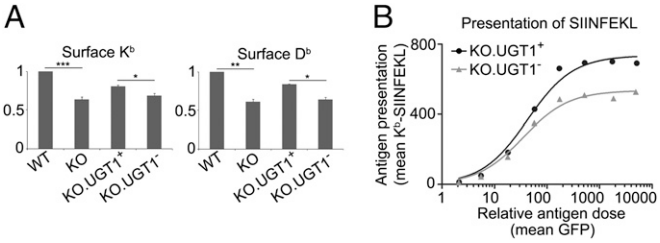

Fig. 2. MHC class I antigen presentation is impaired in the absence of UGT1. (*A*) WT, KO, KO.UGT1$^+$, and KO.UGT1$^-$ cells were stained for surface K^b/β_2m (Y3) (*Left*) and D^b/β_2m (B22) (*Right*) for FACS analysis. Data shown are mean ± SD of two or three experiments. $*P < 0.05$, $**P < 0.01$, $***P < 0.001$. (*B*) Presentation of SIINFEKL by K^b is impaired in the absence of UGT1. Twenty-four hours after the construct encoding GFP-ubiquitin-SIINFEKL was transfected into KO.UGT1$^+$ and KO.UGT1$^-$, cells were stained for K^b/β_2m/SIINFEKL trimer (25-D1.16) for FACS analysis. Cells were split into eight groups according to the extent of their GFP levels. For each group, the mean 25-D1.16 levels (surface presentation of SIINFEKL) were plotted against the mean GFP levels (the relative antigen dose).

Maturation of MHC Class I Molecules Is Less Efficient in the Absence of UGT1. The different ER-Golgi glycosylation patterns for K^b in KO.UGT1$^+$ vs. KO.UGT1$^-$ cells (Fig. 1*B*) suggested a delay in the maturation of K^b in KO.UGT1$^-$ cells, with more immature K^b molecules in the ER at steady state. To examine the mechanisms underlying this we first performed a pulse-chase analysis to examine the kinetics of transport, using the acquisition of resistance to endoglycosidase H (Endo H) as a measure of transport through the Golgi apparatus. The results showed that transport out of the ER was indeed significantly slower in the absence of UGT1 (Fig. 3*A*). We next asked if the reduction in ER exit rate was a function of prolonged interactions between CNX and K^b, the initial step of postsynthetic K^b maturation. ^{35}S-labeled cells were chased for the indicated times, and extracts immunoprecipitated for CNX. After stripping in SDS, both CNX and K^b were reimmunoprecipitated (Fig. 3*B*). Quantification showed that K^b dissociates from CNX more slowly in KO.UGT1$^-$ than in KO.UGT1$^+$ (Fig. 3*B*). A similar delay was also observed for the kinetics of the dissociation of K^b from CRT (Fig. 3*C*) or from the PLC (Fig. 3*D*).

Because the monoglucosylated N-linked glycan plays an important role in the association between glycoproteins and CNX/CRT, we examined the kinetics of the monoglucosylation status of K^b. Pulse-labeled monoglucosylated K^b was isolated at different time points by first using beads with prebound GST-CRT fusion protein, and then immunoprecipitating released K^b HCs after SDS stripping (Fig. 3*E*). Consistent with the delayed K^b-CNX, K^b-CRT, and K^b-PLC dissociation kinetics, monoglucosylated K^b disappeared more slowly in the absence of UGT1.

MHC Class I Molecules Are Less Stable in the Absence of UGT1. The prolonged ER residence of MHC class I molecules in KO.UGT1$^-$ cells suggested that they might be encountering problems in optimizing the spectrum of associated peptides. A commonly used readout for peptide affinity is the stability of MHC class I complexes (15–17). Two different assays were performed to address this. First, in a biochemical approach, largely following the method described by an earlier study (15), ^{35}S-labeled cell lysates were incubated overnight in the presence or absence of 20-μM SIINFEKL peptide to stabilize suboptimally loaded K^b molecules. Intact K^b/β_2m complexes were then immunoprecipitated using the conformation-sensitive mAb Y3 (Fig. 4*A*). Our findings show that the stability of K^b/β_2m is

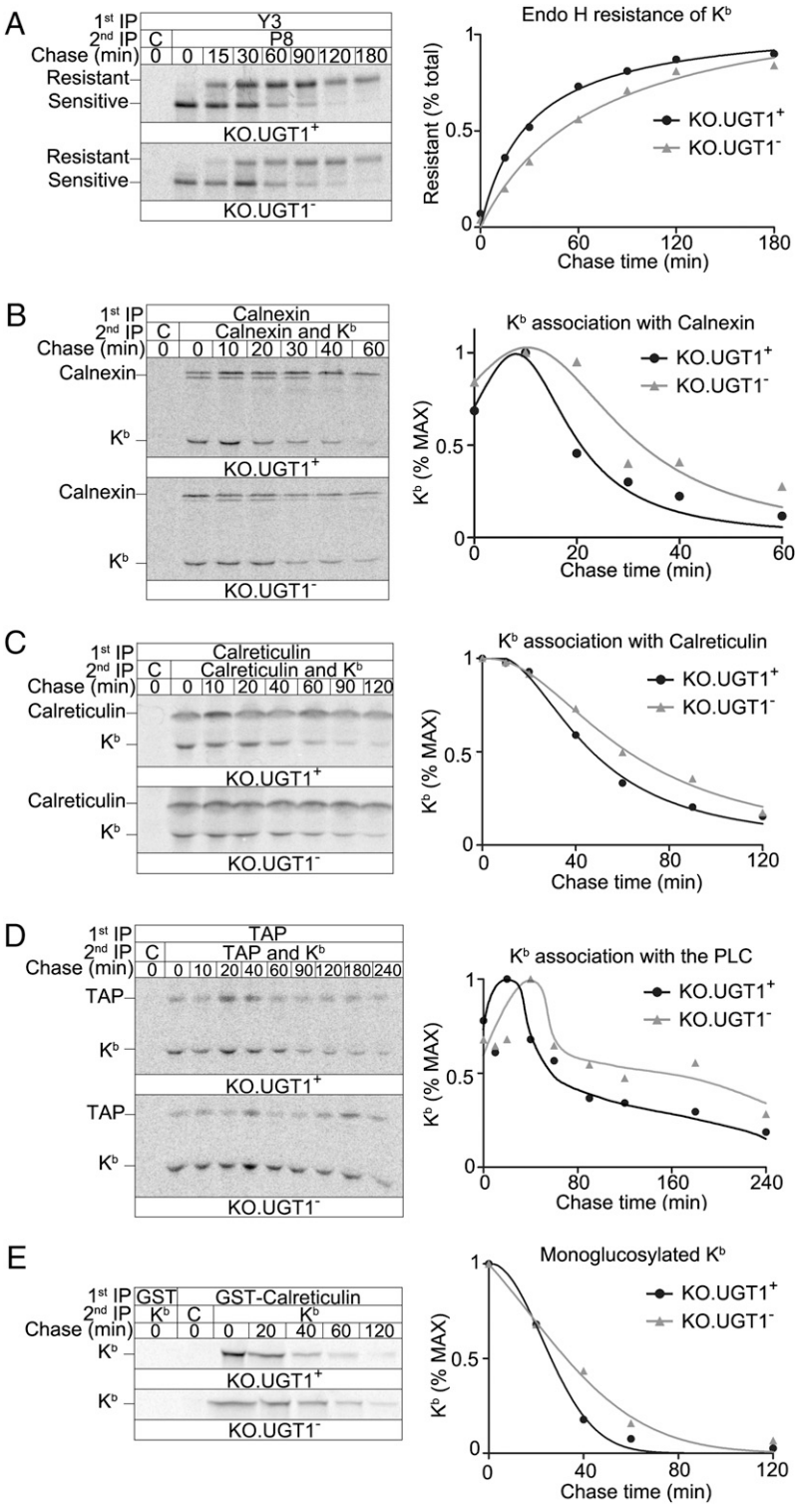

Fig. 3. Maturation of MHC class I molecules is delayed in the absence of UGT1. (*A*) Cells were pulse-labeled for 15 min with ^{35}S-methionine/cysteine, and chased for the indicated times. K^b/β_2m complexes were pulled down with the Y3 antibody. Reimmunoprecipitation with the P8 antibody that recognizes all conformational states of K^b was performed to clear the background for quantification. Immunoprecipitates were digested with Endo H before being separated on SDS/PAGE. (*Right*) Quantification of the export rate, shown as the percentage of the resistant band in the total (resistant and sensitive bands). (*B*) KO.UGT1$^+$ and KO.UGT1$^-$ were pulse-labeled for 10 min, chased for the indicated times, and immunoprecipitated first for CNX using a rabbit antibody, then for both CNX and K^b (the P8 antibody). (*Right*) Percentage of the maximum K^b signal throughout the chase period. (*C* and *D*) Similar to *B*, CRT and TAP with K^b were pulled down, respectively. (*E*) Pulse-labeled monoglucosylated K^b was isolated by first immunoprecipitated using beads with prebound GST-CRT fusion protein or GST as a control, and then reimmunoprecipitated for K^b (P8). (*Right*) The disappearance rate of monoglucosylated K^b during the chase.

significantly reduced in the absence of UGT1, indicating that despite the longer period for folding and peptide loading, peptide selection is suboptimal.

In a second approach, we incubated intact cells overnight in the presence of the K^b-binding peptide SIINFEKL or the D^b-binding peptide ASNENMDAM. Both SIINFEKL and ASNENMDAM can exchange with low-affinity peptides presented by MHC class I molecules on the cell surface and thus stabilize surface MHC class I complexes (17). The fold increase of surface K^b/β_2m and D^b/β_2m complexes was analyzed by flow cytometry using the conformation-specific mAbs Y3 and B22, respectively (Fig. 4 *B* and *C*). In both cases the increase was significantly higher in the absence of UGT1, over a wide range of peptide concentrations. In addition, the expression of K^b/β_2m/SIINFEKL complexes relative to the total K^b was determined using the binding ratio of the 25-D1.16 and Y3 mAbs (Fig. 4*D*). At each concentration of added peptide, a significantly higher fraction of surface K^b/β_2m complexes exchanged their endogenous ligands for SIINFEKL in KO.UGT1$^-$

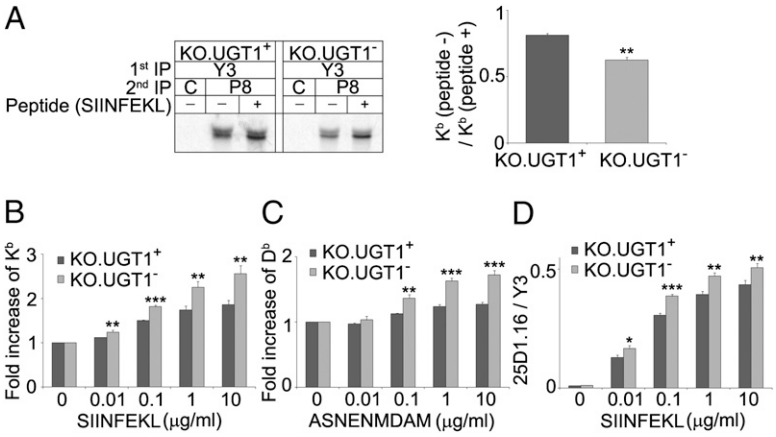

Fig. 4. MHC class I molecules are less stable in the absence of UGT1. (*A*) Cells were labeled with ^{35}S-methionine/cysteine for 1 h, and postnuclear supernatants were incubated overnight at 4 °C in the presence (+) or absence (–) of 20-μM SIINFEKL peptide. K^b/β_2m complexes were isolated by Y3, followed by P8 immunoprecipitation. (*Right*) K^b (no peptide)/K^b (peptide) ratio as mean ± SD of two experiments. $^{**}P < 0.01$. (*B*) Intact cells were cultured overnight with (0.01, 0.1, 1, and 10 μg/mL) or without (0 μg/mL) the K^b-binding peptide SIINFEKL, and then stained for K^b/β_2m (Y3) before FACS analysis. The Y3 signal at each concentration was normalized to the Y3 value where SIINFEKL was not added. Data shown are mean ± SD of three experiments. $^{**}P < 0.01$, $^{***}P < 0.001$. (*C*) Similar to *B*, but with D^b-binding peptide ASNENMDAM and the B22 antibody (D^b/β_2m). Data shown are mean ± SD of three experiments. $^{**}P < 0.01$, $^{***}P < 0.001$. (*D*) Cells were incubated with SIINFEKL as in *B*. Half the cells were stained for K^b/β_2m (Y3), and the other half for K^b/β_2m/SIINFEKL (25-D1.16). The 25-D1.16/Y3 ratio is shown as mean ± SD of three experiments. $^{*}P < 0.05$, $^{**}P < 0.01$, $^{***}P < 0.001$.

cells. Thus, both the biochemical and flow cytometry-based assays demonstrated that the selection of high-affinity ligands by MHC class I molecules is enhanced by UGT1.

UGT1 Preferentially Reglucosylates MHC Class I Molecules Loaded with Suboptimal Peptides. Given the general difficulty in pinpointing a direct role for UGT1 in cellular studies, we adopted a cell-free system using purified recombinant *Drosophila* UGT, a homolog of human UGT1, and MHC class I molecules to address this. Because the cell-free system in our laboratory has been optimized for the human MHC class I allele HLA-B8 (see companion paper, ref. 3), we first asked whether HLA-B8 expression would be affected by the absence of UGT1 in MEFs. KO.UGT1$^+$ and KO.UGT1$^-$ cells were transduced with MSCV-HLA-B8-IRES-GFP retrovirus vector and sorted for the same expression level of GFP. The HLA-B8 and GFP are translated from a single bicistronic mRNA, and the identical expression levels of GFP in both cell types indicate that HLA-B8 is synthesized at the same rate. Despite this, the surface levels of HLA-B8 were lower in KO.UGT1$^-$.B8 than in KO.UGT1$^+$.B8 cells (Fig. 5*B*), as was observed for the endogenous mouse MHC class I molecules (Fig. 2*A*).

We previously established a panel of peptides with different affinities for HLA-B8 (18). Two of them, the high-affinity influenza A virus peptide NP (380-387L) and the intermediate-affinity peptide RAL, a variant of the antigenic peptide EBNA3 (339-447), henceforth referred to as NP and RAL, were used to generate either optimally or suboptimally loaded MHC class I molecules to serve as substrates of recombinant UGT in a subsequent reglucosylation assay. Briefly, we purified HLA-B8 in the presence of the intermediate-affinity RAL peptide. The HLA-B8/RAL complex was further incubated with either the high-affinity peptide NP to drive peptide exchange or again with the RAL peptide, resulting in HLA-B8/NP or HLA-B8/RAL complexes, as expected (Fig. S2). The complexes were then incubated with purified UGT and [^{3}H]UDP-glucose at 30 °C for 1 h before immunoprecipitation of HLA-B8 and quantitation of the ^{3}H signal. Strikingly, UGT exhibited a strong selectivity (>12-fold) toward HLA-B8 associated with the intermediate-affinity peptide RAL vs. that associated with the high-affinity peptide NP (Fig. 5*D*). This suggests that UGT1 indeed acts as a sensor for the quality of the MHC class I-associated peptide cargo and that, in vivo, selective reglucosylation of suboptimally loaded MHC class I molecules may drive them back into the PLC for peptide exchange and affinity optimization.

Discussion

UGT1 is an ER-resident enzyme that monitors glycoprotein folding by retaining incompletely folded/assembled glycoproteins in the CNX/CRT cycle (9). In this study, we uncovered a unique level of quality control of MHC class I antigen presentation mediated by UGT1. In the absence of UGT1, despite seemingly unaffected PLC formation, the surface levels of MHC class I are reduced, class I maturation is delayed, and the peptide repertoire presented by MHC class I molecules is impaired. Most interestingly, we find that *Drosophila* UGT preferentially recognizes and reglucosylates MHC class I loaded with suboptimal peptides. These reglucosylated MHC class I molecules carrying suboptimal peptides can be recruited into the PLC to undergo peptide exchange and loading with high-affinity peptides (3). Based on these data, we hypothesize that after MHC class I molecules dissociate from the PLC, GlsII deglucosylates the monoglucosylated class I, preventing immediate reassociation with the PLC. UGT1, however, preferentially recognizes and reglucosylates MHC class I with suboptimal peptides, which then get recruited back into the PLC for peptide optimization. Conceivably "empty" heterodimers, present in the experiment shown in Fig. 5*C* at a higher

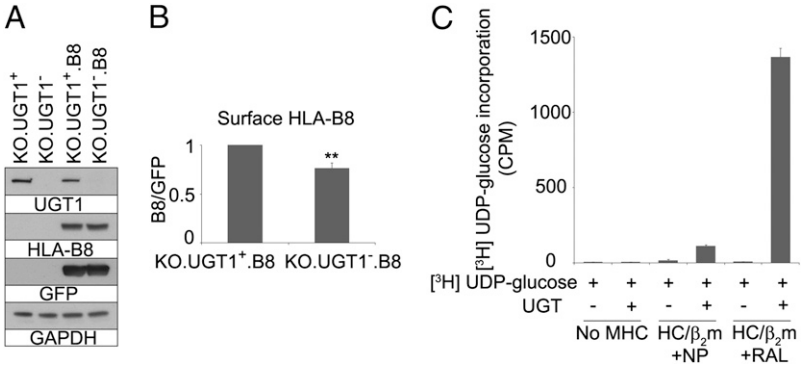

Fig. 5. UGT1 preferentially reglucosylates MHC class I molecules loaded with suboptimal peptides. (*A*) KO.UGT1$^+$, KO.UGT1$^-$, KO.UGT1$^+$ expressing HLA-B8 (KO.UGT1$^+$.B8) and KO.UGT1$^-$ expressing HLA-B8 (KO.UGT1$^-$.B8) were blotted for UGT1, HLA-B8 (3B10.7), GFP, and GAPDH as a loading control. (*B*) KO.UGT1$^+$.B8 and KO.UGT1$^-$.B8 were stained for surface HLA-B8 before FACS analysis. Data shown are mean ± SD of three experiments. $^{**}P < 0.01$. (*C*) HLA-B8 preloaded with the high-affinity peptide NP or the intermediate-affinity peptide RAL was incubated with purified *Drosophila* UGT and [^{3}H]UDP-glucose for 1 h at 30 °C. An excess of unlabeled UDP-glucose was added at the end of the incubation. Samples were immunoprecipitated with w6/32 (anti-MHC class I/β_2m). Elutes were counted for ^{3}H by a liquid scintillation analyzer. The assay was repeated twice with similar results. Data shown are from duplicate samples in one experiment.

equilibrium concentration for the lower-affinity peptide, are the true UGT1 target. This question remains to be answered.

Our cell-based analyses showed a significantly impaired peptide repertoire in the absence of UGT1 (Fig. 4) likely not solely because of a defect in the assembly of MHC class I HC with β_2m. Adding exogenous peptides into the cell culture medium was able to stabilize surface HC/β_2m and raise the surface class I level in KO.UGT1$^-$ cells to a level that is not significantly different from that in KO.UGT1$^+$ cells. Also unlikely is an indirect effect of the lack of UGT1 on PLC formation (Fig. 1 *B* and *C*). Our cell-free system suggests that UGT1 may have the ability to distinguish subtle conformational differences between class I molecules with optimal or suboptimal peptides. Such differences, although poorly defined and still controversial, have been previously suggested (19, 20). Notably, UGT from *Drosophila*, used in the experiments reported here, has the ability to differentiate between MHC molecules loaded with optimal and suboptimal peptides. This argues that the discriminatory capacity is not an evolved function of the mammalian enzyme, but rather results from the normal chaperone-like function of UGT.

Different peptides confer different levels of stability onto MHC class I molecules (e.g., half-life and T_m), variations arising from the length of the peptides, a collection of hydrogen bonds, and how well anchor residues fit into the hydrophobic pockets in the binding groove, etc. Importantly, this stability is correlated with the ability of MHC class I-peptide complexes to trigger T-cell responses in vitro and in vivo (21). In line with the instability of empty MHC class I molecules, extensive data have supported conformational changes in the peptide-binding groove of MHC class I molecules upon peptide binding. In addition, peptide-specific conformational changes have been supported by peptide-specific generation of conformational epitopes that can be differentiated by antibodies (19) and peptide-specific increase in half-life/T_m (22, 23). Although several studies have failed to identify major conformational differences in crystal structures of MHC class I molecules associated with suboptimal vs. optimal peptides (24–26), T-cell receptors can discriminate between such complexes (20). This strongly suggests that conformational differences do exist, but are likely too subtle or dynamic to be revealed by X-ray crystallography.

How UGT1 recognizes conformational perturbations in its substrates is poorly understood. The N-terminal domain, consisting of 75% of this 174-kDa protein, is believed to possess the sensing function (27). This domain has low similarity among species and shares no homology to any other protein known so far. It has been proposed that UGT1 recognizes solvent-accessible hydrophobic patches together with the core pentasaccharide Man3GlcNAc2 (28). The requirement for the distance between N-glycan and conformational disorder is controversial. Some studies suggest that reglucosylation occurs only in glycans near the conformational perturbation (12), and another study found that the distance could be as far as 40 Å (29). MHC class I HC consists of three domains: α1 and α2 domains fold into the peptide-binding groove, and α3 associates with β_2m. All of the MHC class I HCs identified so far have a conserved N-glycosylation site at position 86 (N86) in the α1 domain, which in human MHC class I HCs is the only N-glycosylation site. Murine MHC class I HCs have a second conserved N-linked glycan in the α2 domain (30), and some murine class I HCs have a third site in the α3 domain. N86 resides in the α1 domain outside the peptide-binding groove, near the C-terminal end of the peptide. If UGT1 has a sensing range of 40 Å (29), it would in principle be able to scan the full length of the peptide-binding groove. Molecular dynamic modeling suggests that the region that binds the peptide C terminus is more flexible in the empty state than the corresponding region interacting with the peptide N terminus (31). The empty N-terminal region adopts a "preformed" conformation that is similar to the occupied state (31) and can be largely satisfied by solvents like water in crystal structures (24, 26). In contrast, the empty C-terminal region shows much more fluctuation (31), and it has been proposed that the interaction between the F pocket in the C-terminal region, which is near N86, and the C terminus of the bound peptide is most critical for stabilizing MHC class I molecules (26). Intriguingly, the α2-1 helix, which is in the C-terminal peptide region, is involved in the interaction between HC and tapasin (32).

Surprisingly, the kinetics of MHC class I maturation are delayed in the absence of UGT1. Similar delays have been observed for a number of glycoproteins, including influenza virus hemagglutinin, both for glucose trimming (33) and substrate release from CNX (13). The reason for this delay is poorly understood. Upon closer examination, the structures of hemagglutinin folding intermediates differ slightly in the presence or absence of UGT1 (13). This delay is even more surprising in the context of MHC class I molecule K^b, because K^b is believed to be a strong "escaper" from the ER quality control machinery (4). Unstable K^b molecules with suboptimal peptides exit the ER either more rapidly [e.g., in the absence of CRT (17) or ERp57 (34)] or normally (e.g., in the absence of tapasin) (35), leading to impaired antigen presentation. It is possible that some conformational defects can be recognized by other chaperones (e.g., CNX, CRT, and potentially tapasin, as suggested by the experiments in Fig. 3) when UGT1 is not monitoring the folding status, and that this leads to delayed kinetics. Alternatively, UGT1 or a UGT1-associated protein, such as the oxidoreductase Sep15 (36), may play an as-yet-unidentified role. However, although elements of the precise mechanism remain to be uncovered, our data show that in addition to the well-established quality control machinery of MHC class I antigen presentation involving tapasin and the PLC, UGT1 contributes to improving the bound peptide repertoire. Recognition and reglucosylation of MHC class I molecules with suboptimal peptides can lead to their recruitment to the PLC for further peptide exchange and optimization.

Materials and Methods

Cell Lines and Antibodies. UGT1-deficient MEFs and their cognate WT were kind gifts from Maurizio Molinari (Institute for Research in Biomedicine, Bellinzona, Switzerland) (13). Mouse UGT1 was amplified from total RNA extract from WT MEFs and cloned into the expression vector MSCV-IRES-Thy1.1. UGT1-deficient MEFs were transduced with MSCV-UGT1-IRES-Thy1.1 or MSCV-IRES-Thy1.1 vector by spinfection and sorted for Thy1.1 using a FACS Vantage SE. KO.UGT1$^+$ and KO.UGT1$^-$ cells were further transduced with MSCV-HLA B8-IRES-GFP and sorted for GFP. For all experiments, cells were treated with 200 U/mL mouse IFN-γ (R&D Systems) for 24 h before harvesting. Antibodies used in this paper include Y3 (anti-K^b/β_2m) (17), B22 (anti-D^b/β_2m) (17), 25-D1.16 (anti-K^b/β_2m/SIINFEKL) (17), P8 (rabbit anti–all conformational states of K^b) (6), w6/32 (mAb to human MHC class I complexes) (18), 3B10.7 (mAb to human MHC class I HC) (18), rabbit anti-mouse tapasin and rabbit anti-mouse TAP1 (kind gifts from Ted Hansen, Washington University School of Medicine, St. Louis), rabbit anti-TAP1 (M18; Santa Cruz), rabbit anti-CRT (PA3-900; Stressgen), R.p57 (rabbit anti-human ERp57), Clyde (rabbit anti-CNX) (37), rabbit anti-UGT1 (VAP-PT068; Stressgen), mAb anti-GAPDH (6C5; Research Diagnostics), and allophycocyanin-conjugated anti-human HLA-ABC (555555; BD Biosciences).

Pulse-Chase Analyses, Immunoprecipitation, and Western Blotting. Starved cells were pulse labeled with [^{35}S]-methionine/cysteine (PerkinElmer Life Sciences) and chased for the indicated times. For immunoprecipitation, cells were extracted in 1% digitonin (Calbiochem) or 1% Triton X-100 (Sigma) in TBS [0.15 M NaCl, 0.01M Tris (pH 7.4)] containing 1 mM $CaCl_2$ and protease inhibitor mix. Proteins were isolated using the indicated antibodies or 8 μg GST or GST-CRT fusion protein immobilized on glutathione beads for 1.5 h at 4 °C. Isolated proteins were eluted in reducing sample buffer or eluted with glycoprotein denaturing buffer and digested with Endo H (New England Biolabs) overnight. When reprecipitation was required, isolates were eluted in 1% SDS and then diluted into 1% Triton X-100 in TBS, and reimmunoprecipitated for 1 h at 4 °C. Quantification was conducted using ImageQuant software (GE Healthcare).

For immunoblotting, cells were solubilized in 1% Triton X-100 in TBS. For Fig. 1*C*, to prevent thiol-disulfide exchange during experimental procedures, methyl methanethiosulfonate (MMTS; 10 mM final concentration; Pierce) was added to the lysis buffer.

Antigen Presentation Assay and FACS Analysis. The antigen presentation assay was performed as described previously (38). Briefly, cells were transduced with a plasmid encoding GFP-ubiquitin-SIINFEKL (a kind gift from Jacques Neefjes, the Netherlands Cancer Institute, Amsterdam) and stained with mAb 25-D1.16 (anti-K^b/β_2m/SIINFEKL) before FACS.

Reglucosylation of MHC Class I Molecules. The peptides NP and RAL were synthesized by GenScript. HLA-B8 was purified from insect cells in the presence of the intermediate-affinity peptide RAL as described (3). HLA-B8/RAL was incubated with the high-affinity peptide NP for peptide exchange or again with the intermediate-affinity peptide RAL (100 μM) as a mock control (18) for 2 h at 30 °C. Purified β_2m (0.25 mg/mL) was also added to stabilize HLA-B8. The HLA-B8/RAL and HLA-B8/NP complexes were further incubated individually with purified *Drosophila* UGT (1 μM; a kind gift from Karin Reinisch, Yale University, New Haven, CT) and [^{3}H]UDP-glucose (100 μM; Amersham Biosciences) for 1 h at 30 °C. An excess of unlabeled UDP-glucose was added afterward to avoid further labeling. Samples were immunoprecipitated by w6/32 (anti-MHC class I/β_2m), and eluates were counted for ^{3}H using a liquid scintillation analyzer (Perkin-Elmer).

ACKNOWLEDGMENTS. We thank Drs. M. Molinari, J. Neefjes, T. Hansen, and K. Reinisch for valuable reagents. This work was supported by The Howard Hughes Medical Institute and a Cancer Research Institute fellowship (to R.M.L.).

1. Nössner E, Parham P (1995) Species-specific differences in chaperone interaction of human and mouse major histocompatibility complex class I molecules. *J Exp Med* 181: 327–337.
2. Del Cid N, et al. (2010) Modes of calreticulin recruitment to the major histocompatibility complex class I assembly pathway. *J Biol Chem* 285:4520–4535.
3. Wearsch PA, Peaper DR, Cresswell P (2011) Essential glycan-dependent interactions optimize MHC class I peptide loading. *Proc Natl Acad Sci USA* 108:4950–4955.
4. Peaper DR, Cresswell P (2008) Regulation of MHC class I assembly and peptide binding. *Annu Rev Cell Dev Biol* 24:343–368.
5. Radcliffe CM, et al. (2002) Identification of specific glycoforms of major histocompatibility complex class I heavy chains suggests that class I peptide loading is an adaptation of the quality control pathway involving calreticulin and ERp57. *J Biol Chem* 277:46415–46423.
6. van Leeuwen JE, Kearse KP (1996) Deglucosylation of N-linked glycans is an important step in the dissociation of calreticulin-class I-TAP complexes. *Proc Natl Acad Sci USA* 93:13997–14001.
7. Moore SE, Spiro RG (1993) Inhibition of glucose trimming by castanospermine results in rapid degradation of unassembled major histocompatibility complex class I molecules. *J Biol Chem* 268:3809–3812.
8. Tamura T, Sunryd JC, Hebert DN (2010) Sorting things out through endoplasmic reticulum quality control. *Mol Membr Biol* 27:411–427.
9. Molinari M (2007) N-glycan structure dictates extension of protein folding or onset of disposal. *Nat Chem Biol* 3:313–320.
10. Caramelo JJ, Castro OA, Alonso LG, De Prat-Gay G, Parodi AJ (2003) UDP-Glc: glycoprotein glucosyltransferase recognizes structured and solvent accessible hydrophobic patches in molten globule-like folding intermediates. *Proc Natl Acad Sci USA* 100:86–91.
11. Caramelo JJ, Castro OA, de Prat-Gay G, Parodi AJ (2004) The endoplasmic reticulum glucosyltransferase recognizes nearly native glycoprotein folding intermediates. *J Biol Chem* 279:46280–46285.
12. Ritter C, Quirin K, Kowarik M, Helenius A (2005) Minor folding defects trigger local modification of glycoproteins by the ER folding sensor GT. *EMBO J* 24:1730–1738.
13. Soldà T, Galli C, Kaufman RJ, Molinari M (2007) Substrate-specific requirements for UGT1-dependent release from calnexin. *Mol Cell* 27:238–249.
14. Neijssen J, et al. (2005) Cross-presentation by intercellular peptide transfer through gap junctions. *Nature* 434:83–88.
15. Lewis JW, Neisig A, Neefjes J, Elliott T (1996) Point mutations in the alpha 2 domain of HLA-A2.1 define a functionally relevant interaction with TAP. *Curr Biol* 6:873–883.
16. Williams AP, Peh CA, Purcell AW, McCluskey J, Elliott T (2002) Optimization of the MHC class I peptide cargo is dependent on tapasin. *Immunity* 16:509–520.
17. Gao B, et al. (2002) Assembly and antigen-presenting function of MHC class I molecules in cells lacking the ER chaperone calreticulin. *Immunity* 16:99–109.
18. Wearsch PA, Cresswell P (2007) Selective loading of high-affinity peptides onto major histocompatibility complex class I molecules by the tapasin-ERp57 heterodimer. *Nat Immunol* 8:873–881.
19. Catipović B, Dal Porto J, Mage M, Johansen TE, Schneck JP (1992) Major histocompatibility complex conformational epitopes are peptide specific. *J Exp Med* 176: 1611–1618.
20. Denkberg G, Klechevsky E, Reiter Y (2002) Modification of a tumor-derived peptide at an HLA-A2 anchor residue can alter the conformation of the MHC-peptide complex: Probing with TCR-like recombinant antibodies. *J Immunol* 169:4399–4407.
21. van der Burg SH, Visseren MJ, Brandt RM, Kast WM, Melief CJ (1996) Immunogenicity of peptides bound to MHC class I molecules depends on the MHC-peptide complex stability. *J Immunol* 156:3308–3314.
22. Cerundolo V, et al. (1991) The binding affinity and dissociation rates of peptides for class I major histocompatibility complex molecules. *Eur J Immunol* 21:2069–2075.
23. Springer S, Doring K, Skipper JC, Townsend AR, Cerundolo V (1998) Fast association rates suggest a conformational change in the MHC class I molecule H-2Db upon peptide binding. *Biochemistry* 37:3001–3012.
24. Khan AR, Baker BM, Ghosh P, Biddison WE, Wiley DC (2000) The structure and stability of an HLA-A*0201/octameric tax peptide complex with an empty conserved peptide-N-terminal binding site. *J Immunol* 164:6398–6405.
25. Borbulevych OY, Baxter TK, Yu Z, Restifo NP, Baker BM (2005) Increased immunogenicity of an anchor-modified tumor-associated antigen is due to the enhanced stability of the peptide/MHC complex: Implications for vaccine design. *J Immunol* 174:4812–4820.
26. Glithero A, et al. (2006) The crystal structure of H-2D(b) complexed with a partial peptide epitope suggests a major histocompatibility complex class I assembly intermediate. *J Biol Chem* 281:12699–12704.
27. Arnold SM, Kaufman RJ (2003) The noncatalytic portion of human UDP-glucose: glycoprotein glucosyltransferase I confers UDP-glucose binding and transferase function to the catalytic domain. *J Biol Chem* 278:43320–43328.
28. Totani K, Ihara Y, Matsuo I, Koshino H, Ito Y (2005) Synthetic substrates for an endoplasmic reticulum protein-folding sensor, UDP-glucose:glycoprotein glucosyltransferase. *Angew Chem Int Ed Engl* 44:7950–7954.
29. Taylor SC, Ferguson AD, Bergeron JJ, Thomas DY (2004) The ER protein folding sensor UDP-glucose glycoprotein-glucosyltransferase modifies substrates distant to local changes in glycoprotein conformation. *Nat Struct Mol Biol* 11:128–134.
30. Lian RH, Freeman JD, Mager DL, Takei F (1998) Role of conserved glycosylation site unique to murine class I MHC in recognition by Ly-49 NK cell receptor. *J Immunol* 161: 2301–2306.
31. Zacharias M, Springer S (2004) Conformational flexibility of the MHC class I alpha1-alpha2 domain in peptide bound and free states: A molecular dynamics simulation study. *Biophys J* 87:2203–2214.
32. Van Hateren A, et al. (2010) The cell biology of major histocompatibility complex class I assembly: Towards a molecular understanding. *Tissue Antigens* 76:259–275.
33. Pearse BR, et al. (2010) The role of UDP-Glc:glycoprotein glucosyltransferase 1 in the maturation of an obligate substrate prosaposin. *J Cell Biol* 189:829–841.
34. Garbi N, Tanaka S, Momburg F, Hämmerling GJ (2006) Impaired assembly of the major histocompatibility complex class I peptide-loading complex in mice deficient in the oxidoreductase ERp57. *Nat Immunol* 7:93–102.
35. Grandea AG, 3rd, et al. (2000) Impaired assembly yet normal trafficking of MHC class I molecules in Tapasin mutant mice. *Immunity* 13:213–222.
36. Labunskyy VM, et al. (2005) A novel cysteine-rich domain of Sep15 mediates the interaction with UDP-glucose:glycoprotein glucosyltransferase. *J Biol Chem* 280: 37839–37845.
37. Hammond C, Helenius A (1994) Quality control in the secretory pathway: Retention of a misfolded viral membrane glycoprotein involves cycling between the ER, intermediate compartment, and Golgi apparatus. *J Cell Biol* 126:41–52.
38. Howe C, et al. (2009) Calreticulin-dependent recycling in the early secretory pathway mediates optimal peptide loading of MHC class I molecules. *EMBO J* 28:3730–3744.